Extreme Arctic sea ice lows investigated with a rare event algorithm

J. Sauer[1], F. Ragone[1,2], F. Massonnet[1], G. Zappa[3]
[1]Earth and Climate Research Center, Earth and Life Institute, Université catholique de Louvain, Belgium
[2]Royal Meteorological Institute of Belgium, Brussels, Belgium
[3]National Research Council of Italy, Institute of Atmospheric Sciences and Climate, Bologna, Italy
jerome.sauer@uclouvain.be

Introduction: Extreme reductions of the pan-Arctic sea ice area

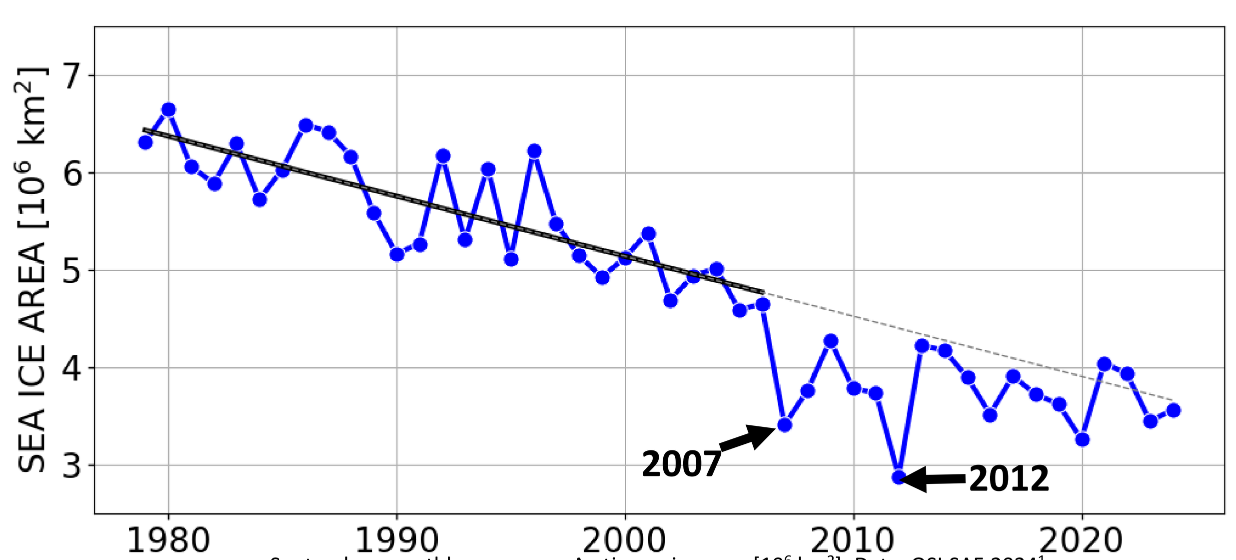

September monthly mean pan-Arctic sea ice area [10^6 km^2]. Data: OSI SAF 2024[1].

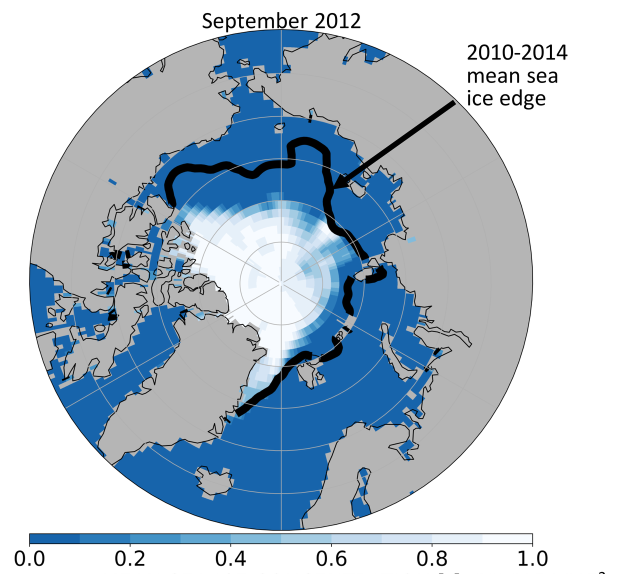

MEAN SEA ICE CONCENTRATION [-] OSI SAF 2017[2].

Goal: Understanding the physical drivers and probabilities of extremes of pan-Arctic sea ice area reduction
→ Preconditioning, sea ice-albedo feedback, oceanic and atmospheric circulations

Problem: quantitative statistical and dynamical studies of climate extremes hindered by lack of data
→ From statistical physics: improve the sampling efficiency of extreme events with rare event algorithms
→ Genealogical selection algorithm adapted from Del Moral and Garnier (2005)[3]; Giardina et al. (2011)[4] (Ragone et al. 2018[5]; Ragone and Bouchet 2019[6]; 2021[7], Sauer et al. 2024[8]): Efficient to study time-persistent extremes

Rare event simulations with PlaSim-T21-LSG: unconditional probability distribution approach

- Independent initial conditions sampled from long control run (stationary pre-industrial climate; (Sauer et al. 2024[8]))
- The algorithm allows to compute return times up to 10^5 years with computational cost of order 10^3 years and enables a statistically robust analysis of extreme sea ice lows with return times of more than 200 years (Figures 2 and 3)

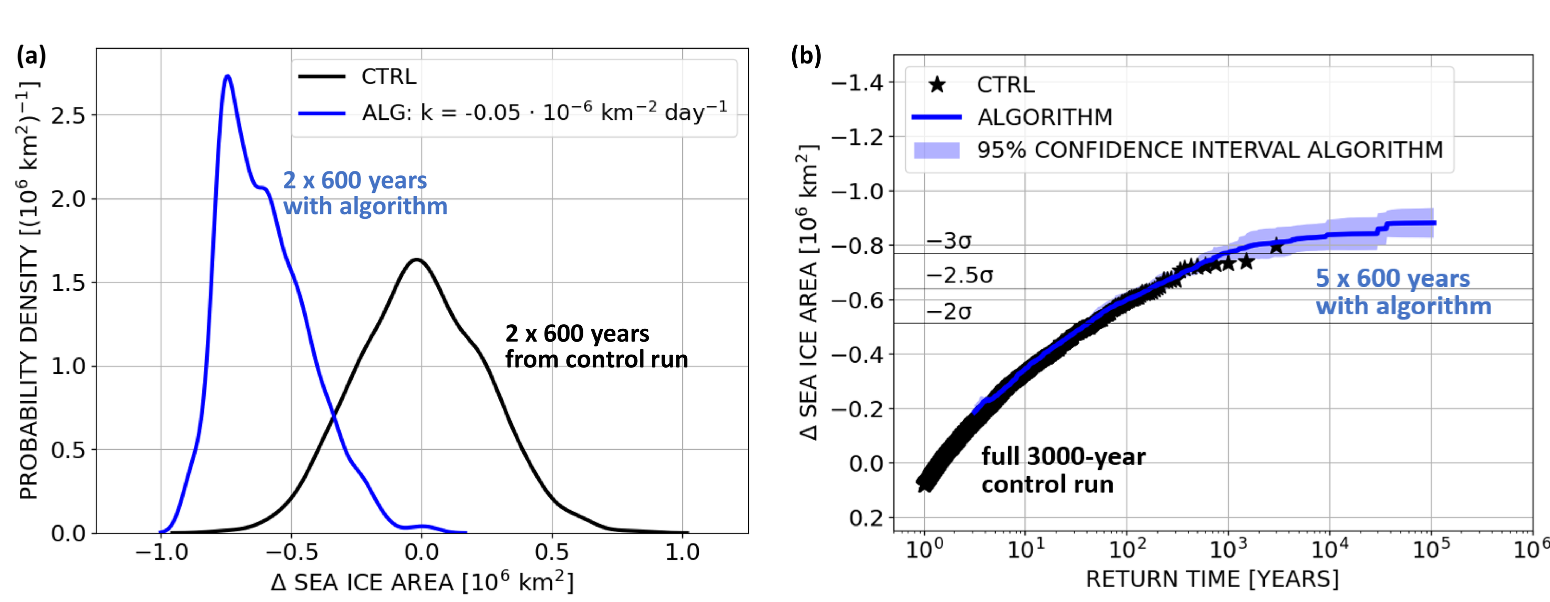

Figure 2: (a) February-September mean pan-Arctic sea ice area anomalies relative to the climatology of the control run for (black) two control ensembles and (blue) two rare event algorithm ensembles. (b) Return times estimated from (black) the control run and (blue) from five ensembles with the rare event algorithm. The blue shading marks the 95% confidence interval.

- Extremely February-September mean Arctic sea ice lows with return times of more than 200 years in PlaSim-T21-LSG associated with
  1) Winter preconditioning in the sea ice-ocean system
  2) Anomalously humid and cloudy Arctic atmosphere throughout late winter and spring
  3) Arctic "heatwave" in early summer 4) Sea ice-albedo feedback

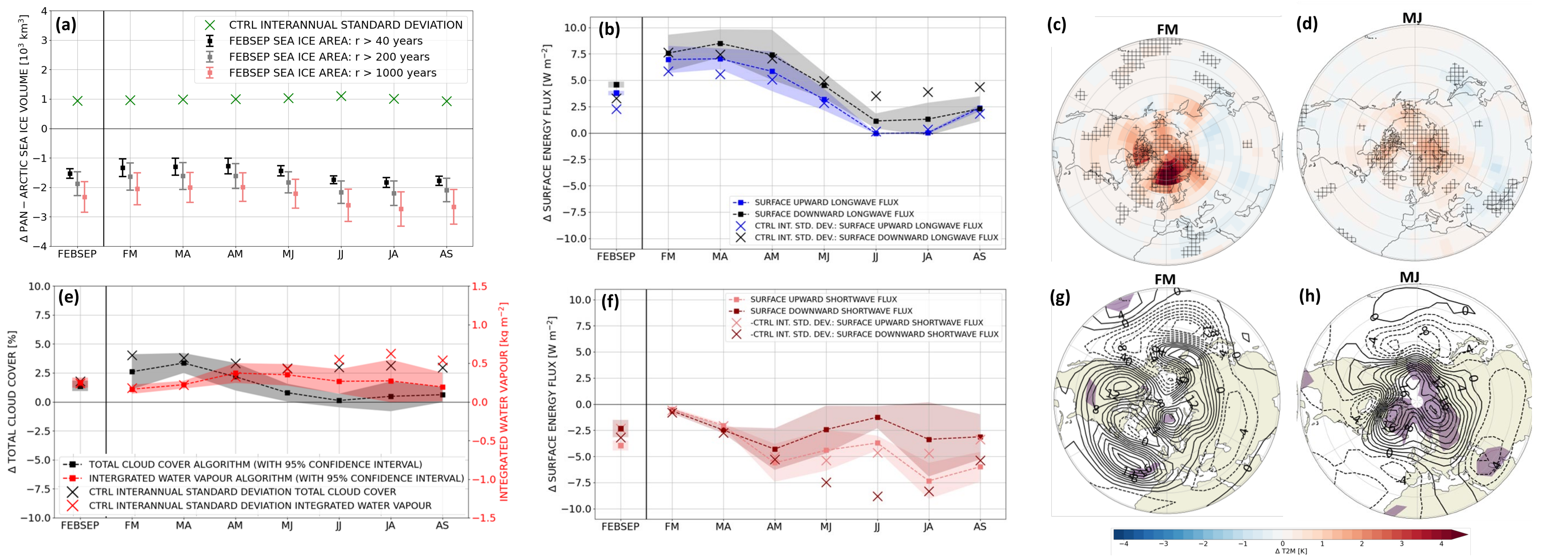

Figure 3: Composites from experiments with the rare event algorithm: (a) Mean pan-Arctic sea ice volume [10^3 km^3] anomalies during seasons of extreme negative February-September (FEBSEP) mean pan-Arctic sea ice area anomalies with return times of more than (black) 40 years, (gray) 200 years and (red) 1000 years. (b,e,f) Mean anomalies of domain-averaged quantities (all ocean grid boxes northern of 70°N) during extremely low sea ice seasons with return times of more than 200 years. Anomalies of (b) the (blue) upward and (black) downward surface longwave radiative flux [W m^{-2}], (e) (black) the total cloud cover [%] and (red) the integrated water vapour [kg m^{-2}] and (f) the (lightcoral) upward and (darkred) downward surface shortwave radiative flux [W m^{-2}]. (b,f) Direction-independent absolute values of the downward and upward radiative fluxes are considered, i.e., a positive (negative) anomaly indicates a radiative flux that is stronger (weaker) in magnitude than the climatology. (c,d,g,h) Composite mean (c,d) 500 hPa geopotential height (Z500 [gpm]; contour interval 2 gpm) anomalies during seasons of extreme negative pan-Arctic sea ice area anomalies with return times of more than 200 years for February-March (FM) and May-June (MJ) and estimated with the rare event algorithm. Shading and error bars in (a,b,e,f) indicate 95% confidence intervals and shading in (f) statistical significance at the 5% level.

Methodology: Rare event algorithm

- Importance sampling of trajectories in ensemble simulation with numerical model
→ Make trajectories leading to large anomalies of a time-averaged observable common
→ Better statistics on extreme events (composites, return times) + generation of ultra-rare events

1) Consider N trajectories $\{X_n(t)\}$ $(n = 1, 2, \ldots, N)$, an observable $A(\{X_n(t)\})$, a total simulation time T_a and a resampling time τ_r
2) At regular times $t_i = i\tau_r$ $(i = 1, \ldots, T_a/\tau_r)$, trajectories are killed or generate a number of replicates depending on the weights

$$w_{n,i} = \frac{e^{k\int_{t_{i-1}}^{t_i} A(\{X_n(t)\})dt}}{R_i}, \quad R_i = \frac{1}{N}\sum_{n=1}^{N} e^{k\int_{t_{i-1}}^{t_i} A(\{X_n(t)\})dt}$$

, with k biasing parameter

3) After the simulation: reconstruction of effective ensemble based on surviving trajectories
4) Importance sampling formula: relates probabilities of trajectories between control simulation and simulation with the rare event algorithm

$$P_k\left(\{X(t)\}_{0\le t\le T_a}\right) = \frac{e^{k\int_0^{T_a} A(\{X(t)\})\,dt}}{R} P_0\left(\{X(t)\}_{0\le t\le T_a}\right)$$

P_k, P_0: prob. dens. in biased and unbiased statistics
k, R: biasing parameter and normalization term
t, T_a: time and simulation length
$A, \{X_n(t)\}$: observable and model trajectories

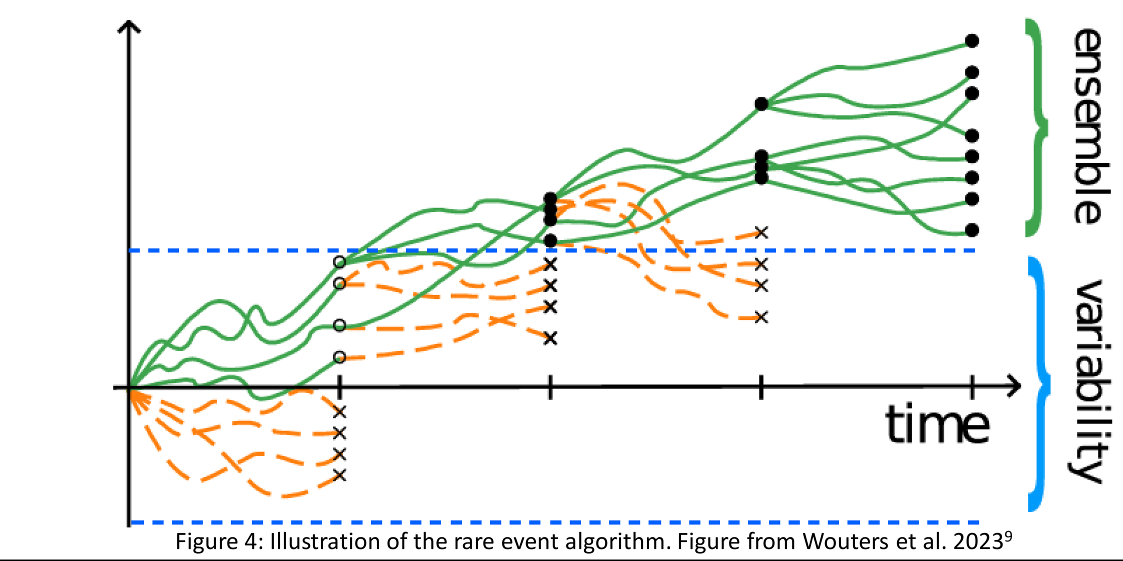

Figure 4: Illustration of the rare event algorithm. Figure from Wouters et al. 2023[9]

Future application of the algorithm to EC-Earth3.3.1

Model version	Resolution	Forcing and initialization
- EC-Earth3.3.1 (Döscher et al. 2022[10]) - IFS-36r4, NEMO-3.6 including LIM3.6	- IFS: T255L91 - NEMO: ORCA1L75	- Fixed greenhouse gas conditions and solar forcing at year 2000 level - Year-2000 NEMO restart files of historical run with EC-Earth3.3.3.2

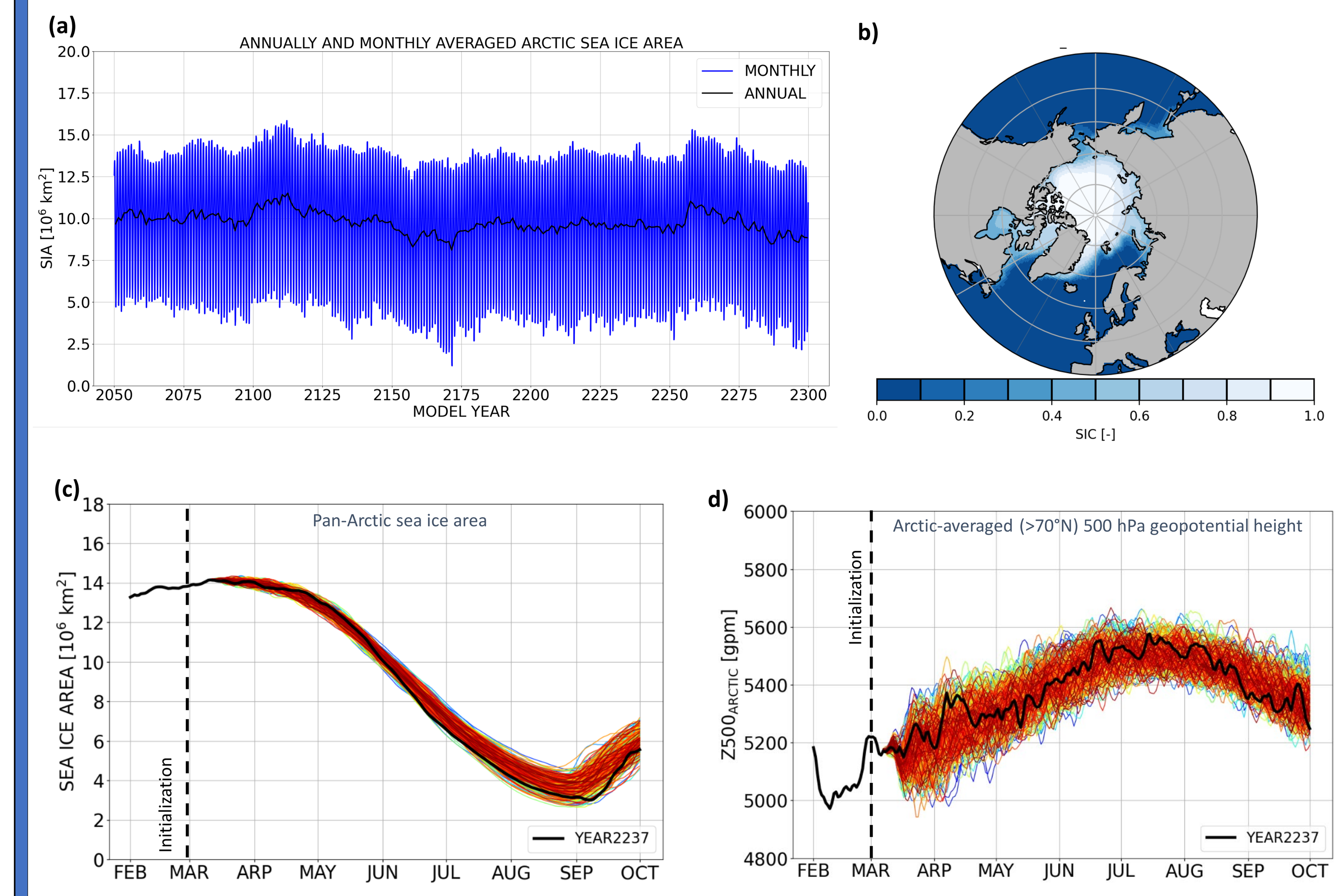

Figure 6: (a) Pan-Arctic sea ice area and (b) annual mean sea ice concentration in EC-Earth3.3.1 control run. The mean sea ice concentration field are computed from model years 2050-2299. (c-d) Control ensemble simulation starting from a neutral sea ice initial condition for the (a) pan-Arctic sea ice area and (b) 500 hPa geopotential height on domain-average northern of 70°N.

- In preparation: two pairs of control and rare event a ensemble simulations (N=300)
  (1) Neutral winter sea ice *vs.*
  (2) 2012-like sea ice initial state via "anomaly initialization"[11]

Rare event simulations with PlaSim-T21-LSG: conditional probability distribution approach

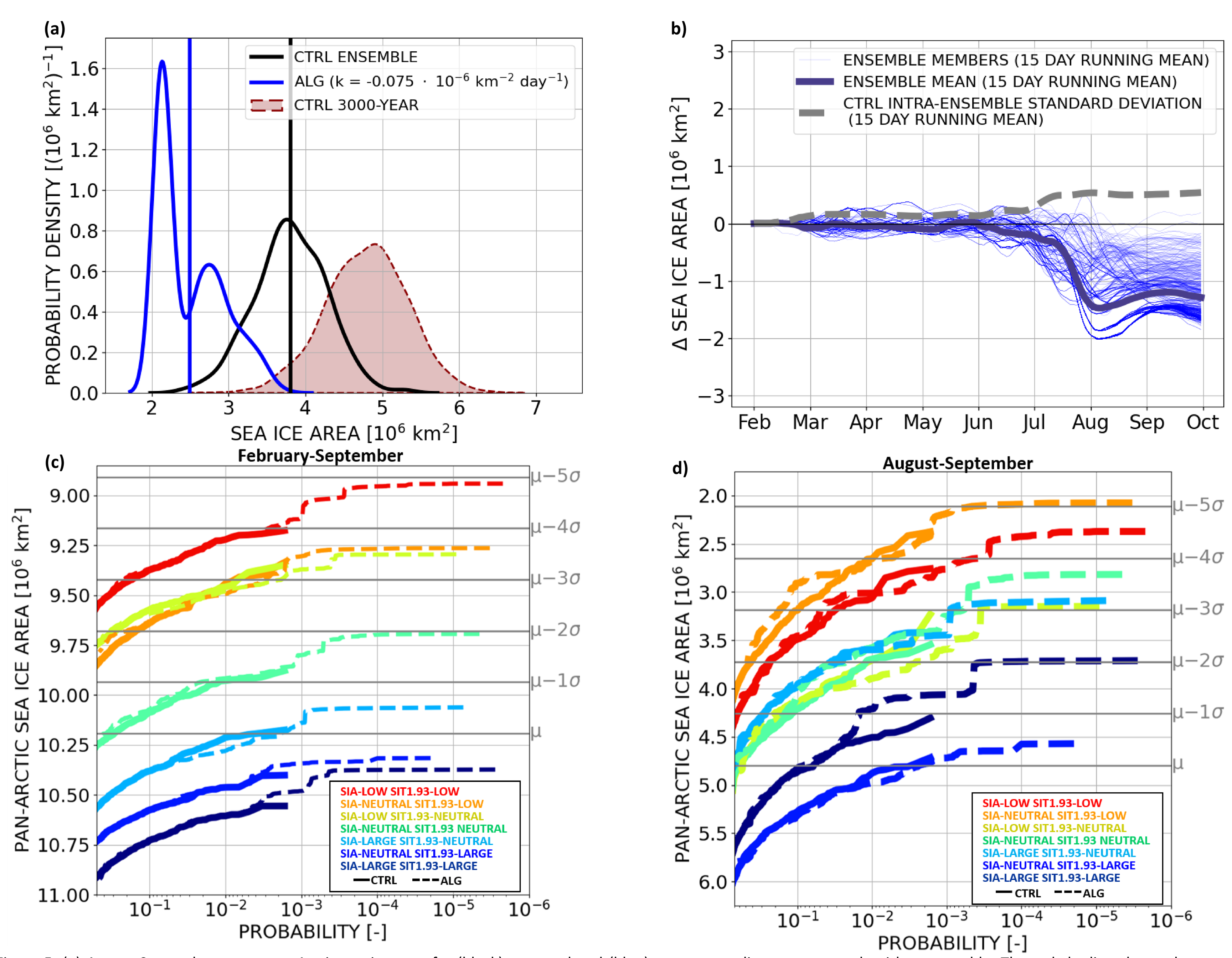

Figure 5: (a) August-September mean pan-Arctic sea ice area for (black) a control and (blue) a corresponding rare event algorithm ensemble. The red shading shows the distribution for a 3000-year control run. (b) As in (a), but for daily sea ice area anomalies obtained with the algorithm and evaluated compared to the control ensemble mean. The gray line indicates the control intra-ensemble standard deviation and the dark blue line the ensemble mean obtained with the rare event algorithm. (c-d) Estimated probabilities (x-axis) of (c) February-September and (d) August-September mean sea ice area values below a given threshold (y-axis) for seven control (solid) and rare event (dashed) ensemble simulations initialized from seven different initial conditions.

- Ensemble simulations initialized from slightly perturbed identitcal initial conditions sampled from control run (stationary pre-industrial climate)
- Seasonal climate prediction set-up: quantification of the probability of an extreme sea ice low as a function of different initial conditions
- The algorithm allows to compute conditional probabilitites of 0.001% for a computational cost of 600 years
- Late summer sea ice area lows are strongly preconditioned by an anomalously low state of the winter cumulative area with sea ice thickness larger than 1.93 metres
- Negligible impact of late winter sea ice area on the probability of an extreme late summer sea ice area low

UCLouvain
Seedfund FSR
fnrs LA LIBERTÉ DE CHERCHER — This communication is supported by the French Community of Belgium as part of a FRIA grant.
EARTH & LIFE INSTITUTE

References

1) OSI SAF 2024, ftp://osisaf.met.no/prod_test/ice/index/v2p2/nh/osisaf_nh_sia_monthly.nc
2) OSI SAF 2017, ftp://osisaf.met.no/reprocessed/ice/conc/v2p0
3) Del Moral, P. and J. Garnier, 2005, https://doi.org/10.1214/105051605000000566
4) Giardina, C., J. Kurchan , V. Lecomte, et al., 2011, https://doi.org/10.1007/s10955-011-0350-4
5) Ragone, F., J. Wouters and F. Bouchet, 2018, https://doi.org/10.1073/pnas.1712645115
6) Ragone, F. and F. Bouchet, 2020, https://doi.org/10.1007/s10955-019-02429-7
7) Ragoen, F. and F. Bouchet, 2021, https://doi.org/10.1029/2020GL091197
8) Sauer, J., J. Demaeyer, G. Zappa, et al., 2024, https://doi.org/10.1007/s00382-024-07160-y
9) Wouters, J., R.K.H. Shiemann and L.C. Shaffrey, 2023, https://doi.org/10.1029/2022MS003537
10) Döscher, R. et al., 2022, https://doi.org/10.5194/gmd-15-2973-2022
11) Tian, T. S. Yang, M. P. Karami, et al., 2021, https://doi.org/10.5194/gmd-14-4283-2021